Supporting Information

Thiazolimines as Novel Ligand-System for Spin-Crossover Centred at Room Temperature

N. Struch, N. Wagner, G. Schnakenburg, R. Weisbarth, S. Klos, J. Beck and A. Lützen

Kekulé-Institut für Organische Chemie und Biochemie, Rheinische Friedrich-Wilhelms-Universität Bonn. Gerhard-Domagk-Straße 1, 53121 Bonn. E-Mail: arne.luetzen@uni-bonn.de

Institut für Anorganische Chemie, Rheinische Friedrich-Wilhelms-Universität Bonn. Gerhard-Domagk-Straße 1, 53121 Bonn.

Synthesis and characterisation

General

All substances were purchased from Alfa Aesar, J. T. Baker, Sigma-Aldrich, or VWR Chemicals and used without further purification. NMR spectra were recorded at 400.1, 300.1 (^{1}H) or 282.4 MHz (^{19}F) with a Bruker Advance DPX 400 or DPX 300 spectrometer. Chemical shifts are given in ppm relative to residual solvent signals (^{1}H). ESI mass spectra were recorded with a Fischer Scientific LTQ Orbitrap XL spectrometer. FT-IR spectra were recorded with a Thermo Nicolet 380 FT-IR spectrometer at room temperature. UV-Vis-spectra were recorded at room temperature using a Jena Analytic Specord 200 spectrometer, a 1 cm quartz cuvette and hplc grade solvents. Temperature-dependent magnetic susceptibility measurements were conducted by using a Quantum Design VSM vibrating sample magnetometer. All experiments were conducted using crystalline material or solutions thereof, respectively, as yielded by the procedures given below. Phase purity was proven by comparison of powder diffractograms with the respective calculated diffractograms calculated from singly crystal XRD-data.

Spectra

^{1}H-NMR of **1**[Cl]$_2$
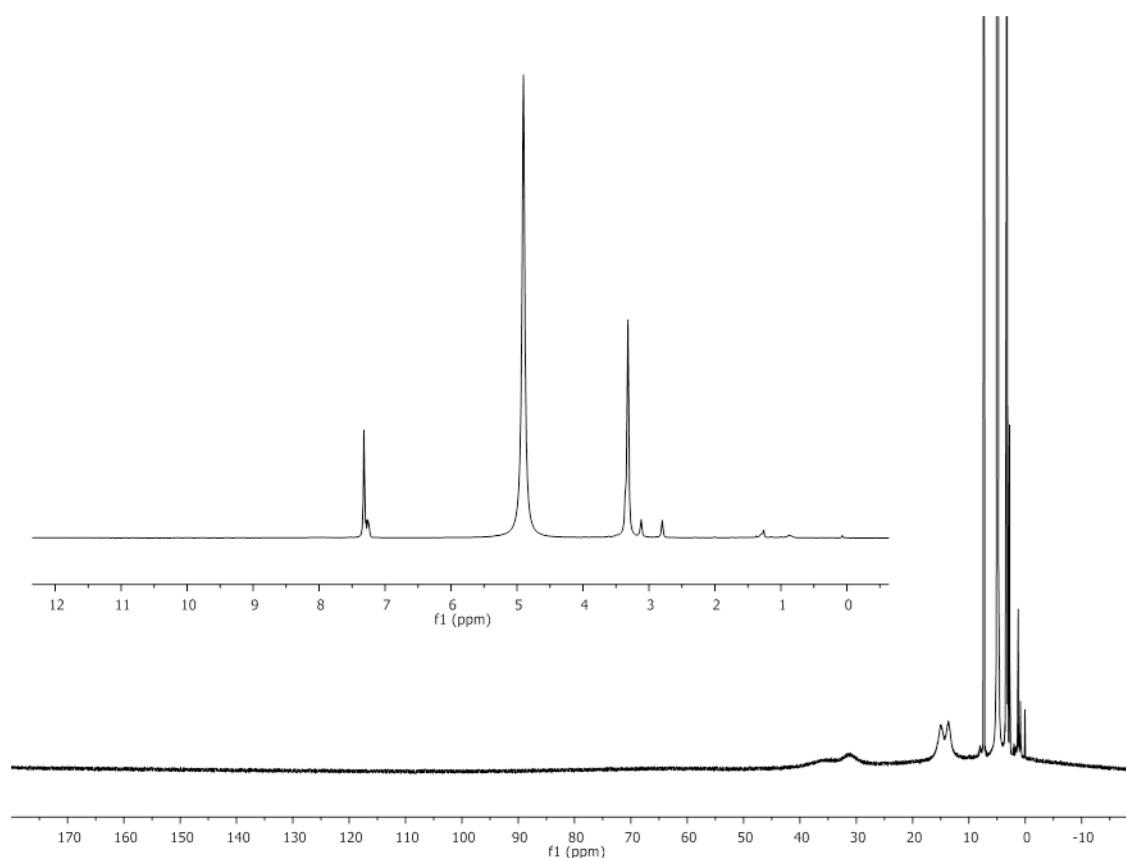
^{1}H-NMR of **1**[Cl]$_2$ (400.1 MHz, MeOH-d_4, 293 K) inset showing the regular NMR regime, scaled to solvent residue signal. The multiplet around 7.3 ppm shows traces of chlorobenzene left from the workup procedure.

*Pos. ESI-HRMS of **1**[Cl]₂*
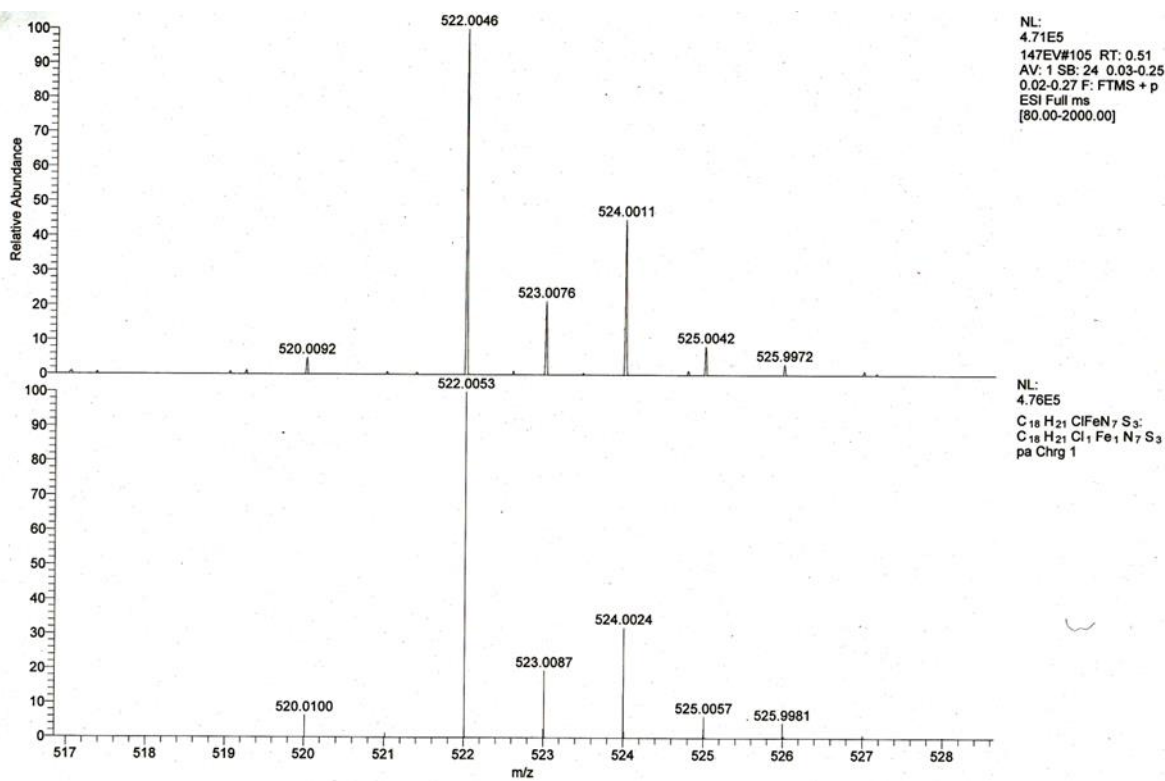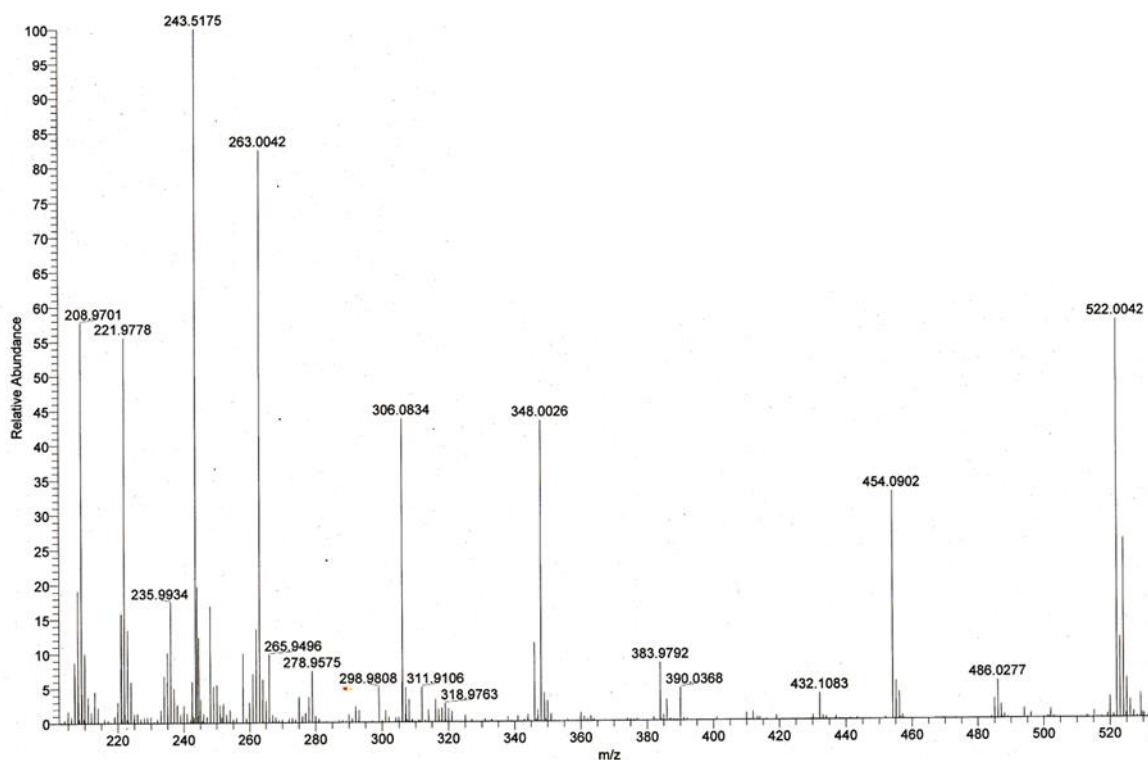
FT-IR-Spectrum of **1**[Cl]₂
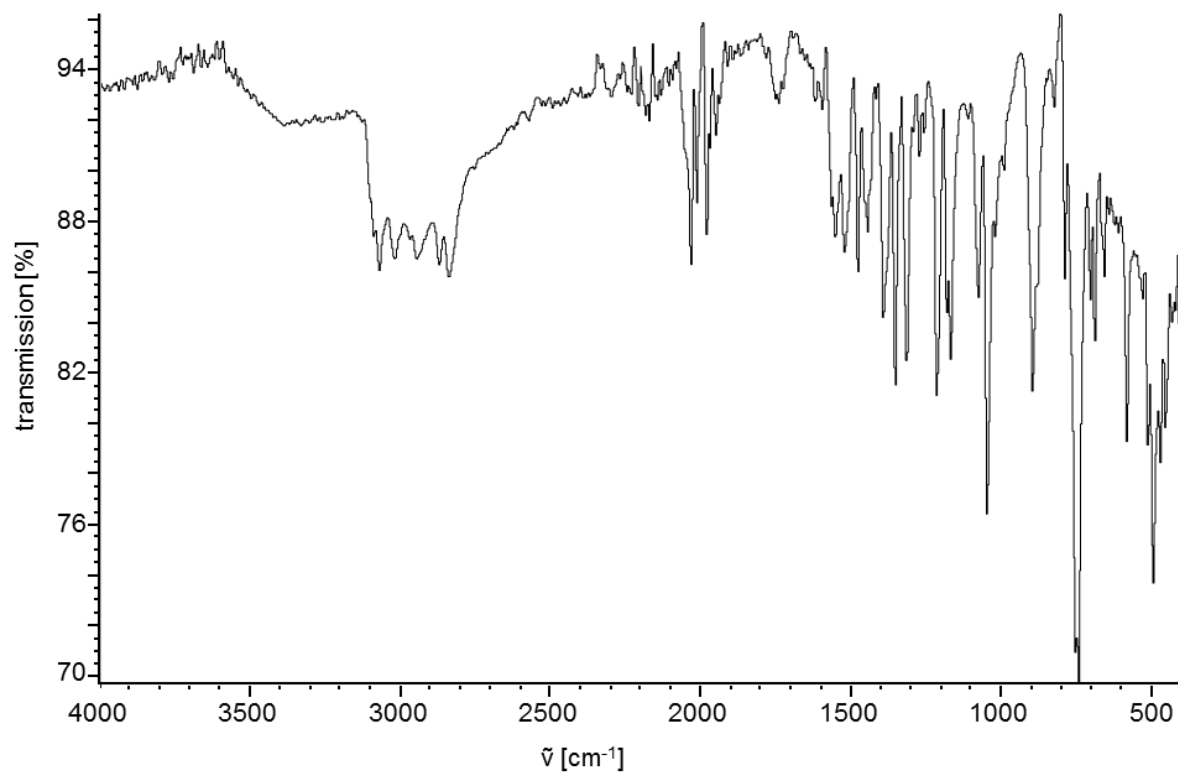
UV/Vis spectrum of **1**[Cl]₂
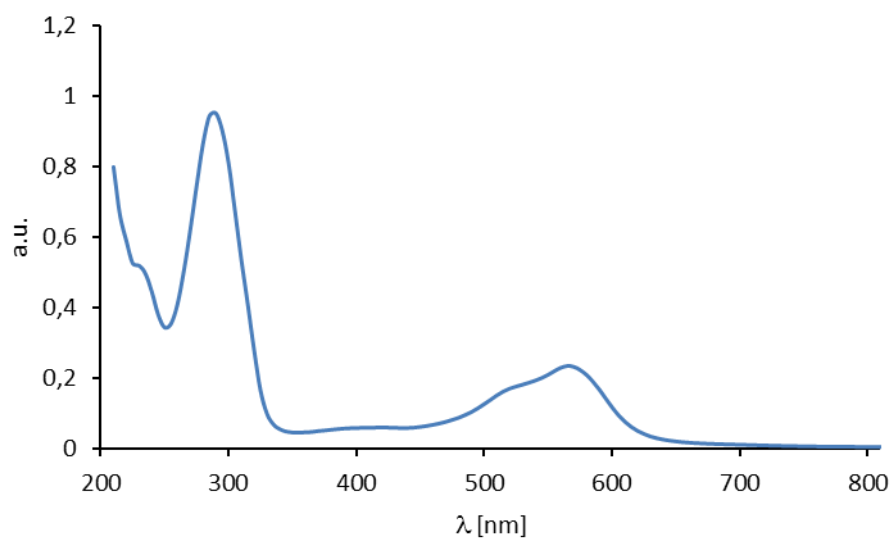
UV/Vis spectrum of **1**[Cl]₂ 50 µM in MeCN.

*¹H-NMR of **1**[SbF₆]₂*
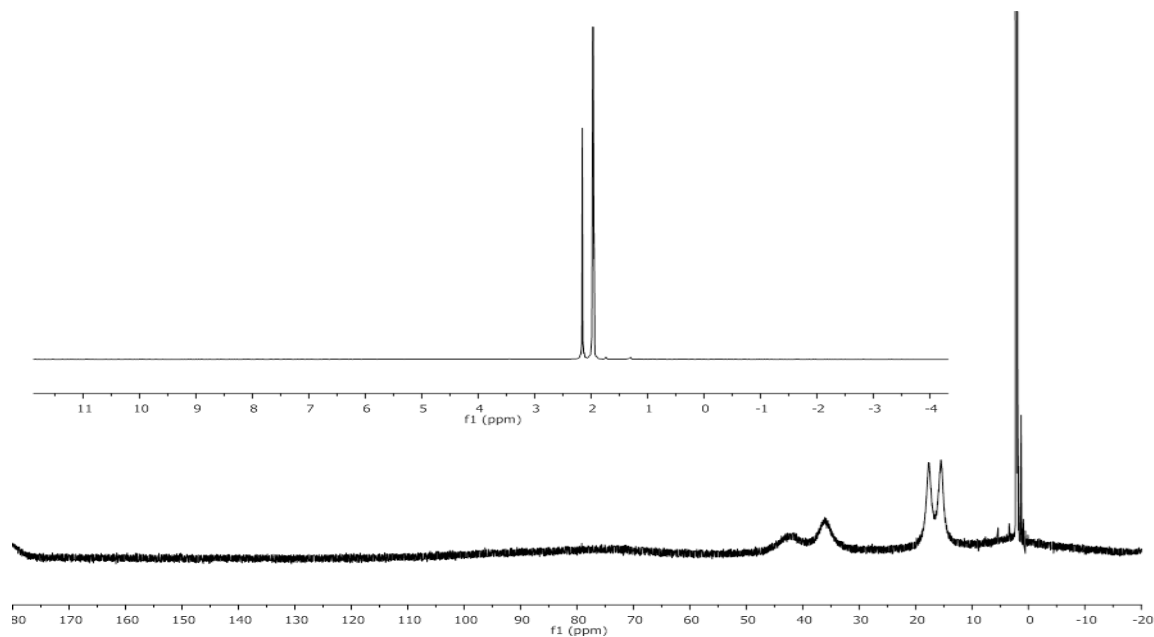
¹H-NMR of **1**[SbF₆]₂ (400.1 MHz, MeCN-d_3, 293 K)

*¹⁹F-NMR of **1**[SbF₆]₂*
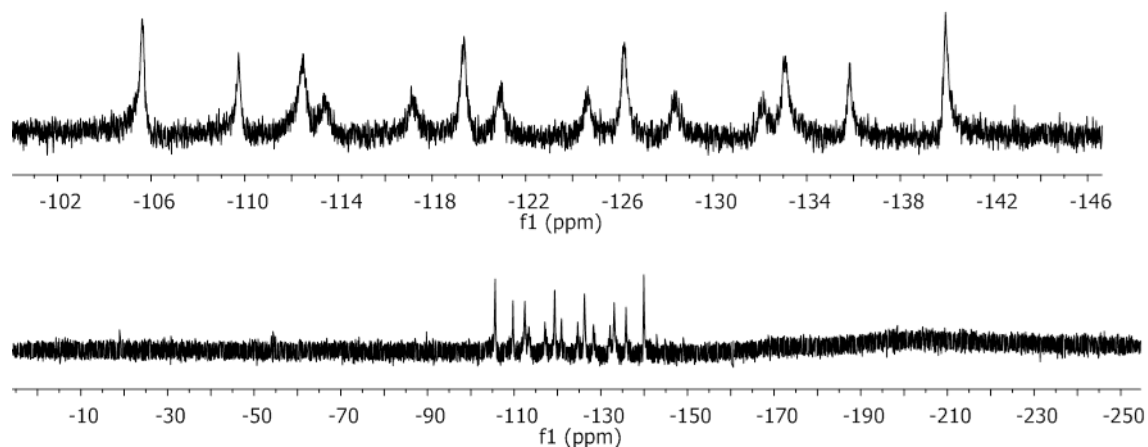
¹⁹F-NMR of a concentrated solution of **1**[SbF6]₂ (282.4 MHz, MeCN-d_3, 293 K). The complicated spectrum arises from two Sb isotopes ¹²¹Sb (S=5/2) and ¹²⁵Sb (S=7/2) and matches the data reported in the literature.[1]

---

[1] R. G. Kidd and R. W. Matthews, *Inorg. Chem.* 1971, **11**, 1156.
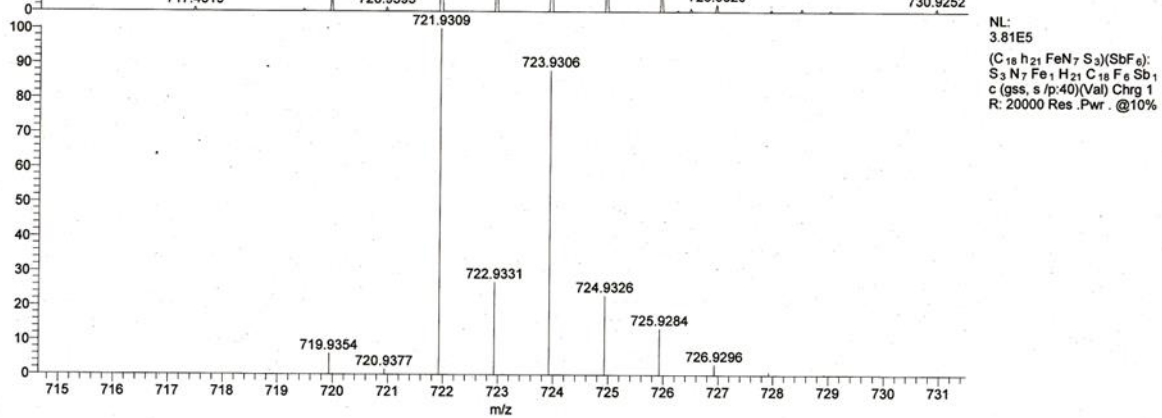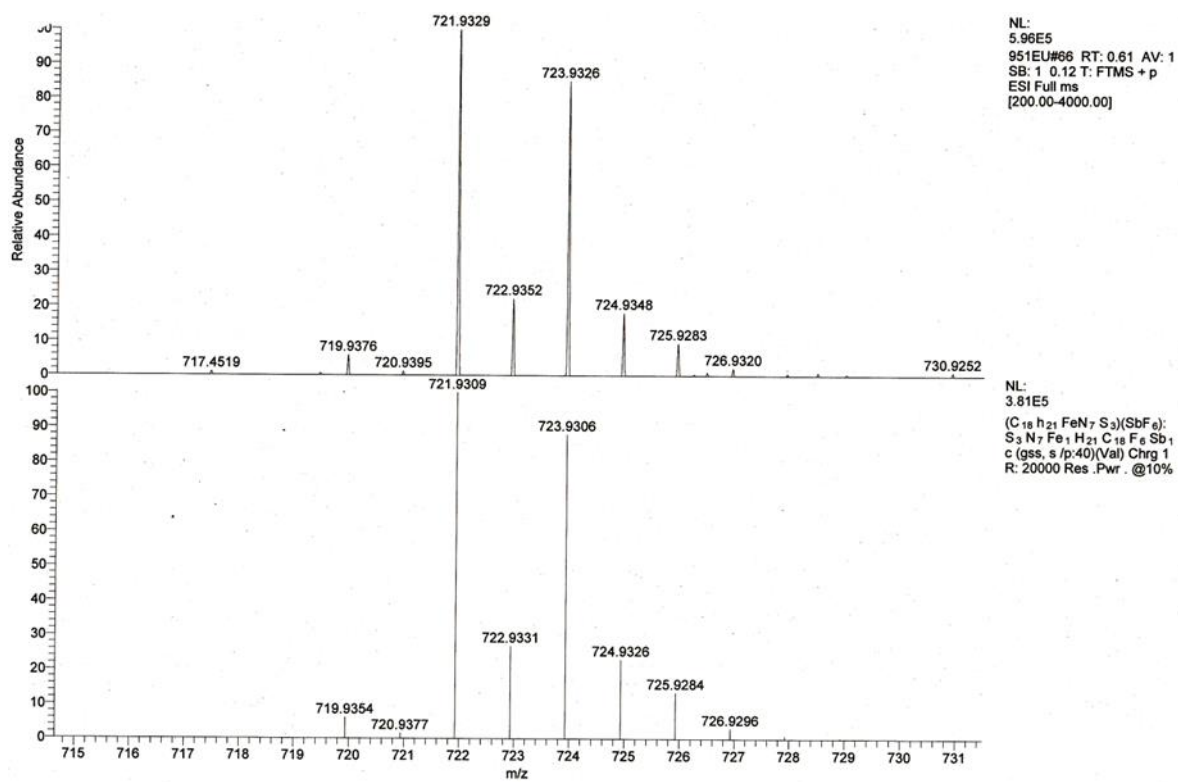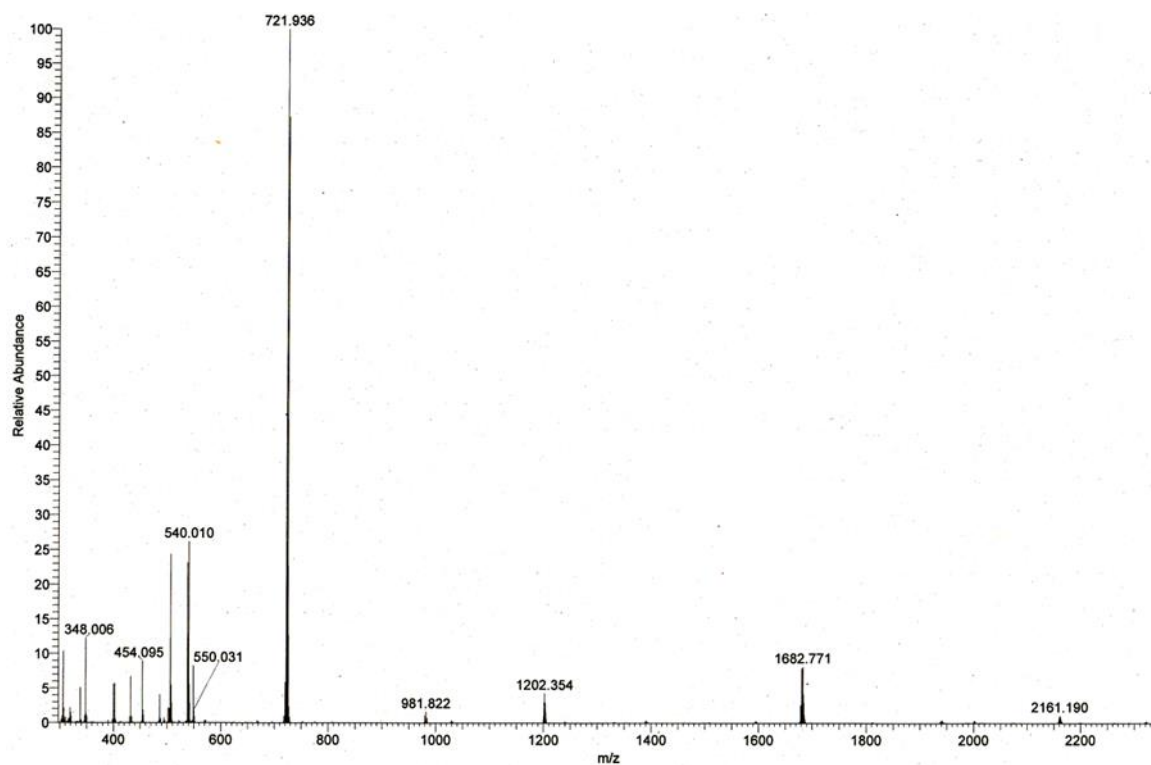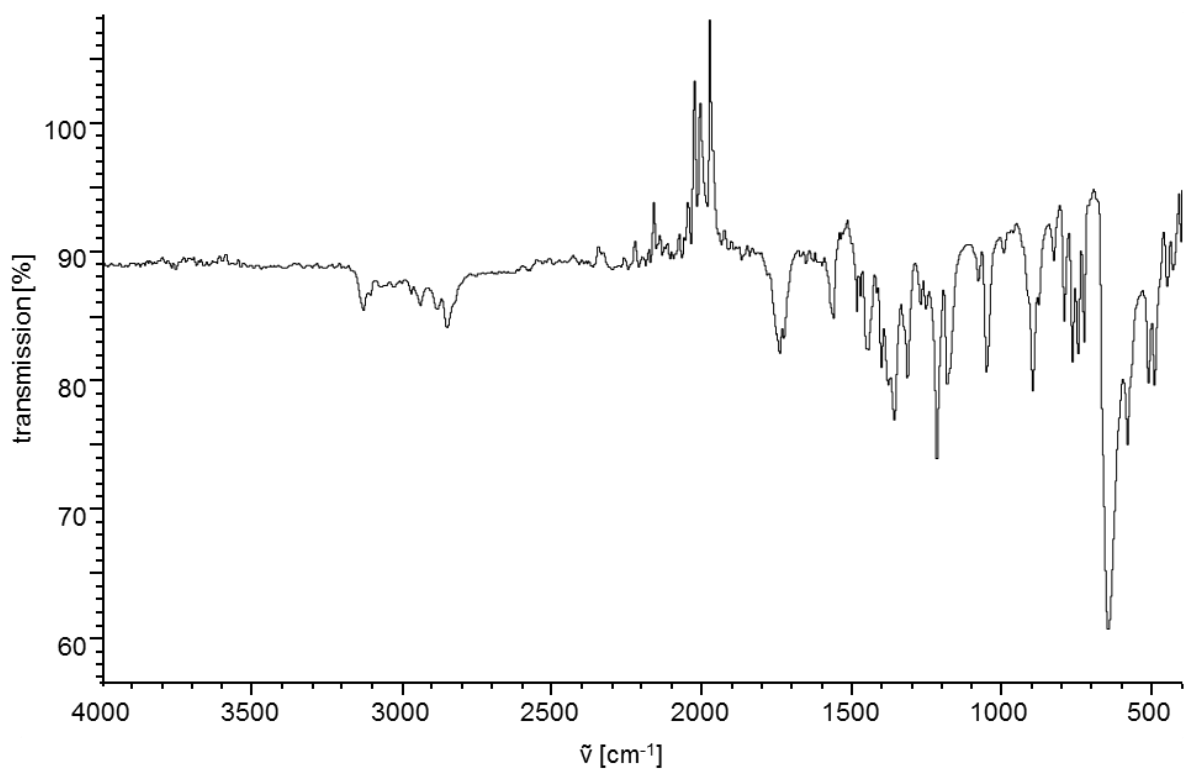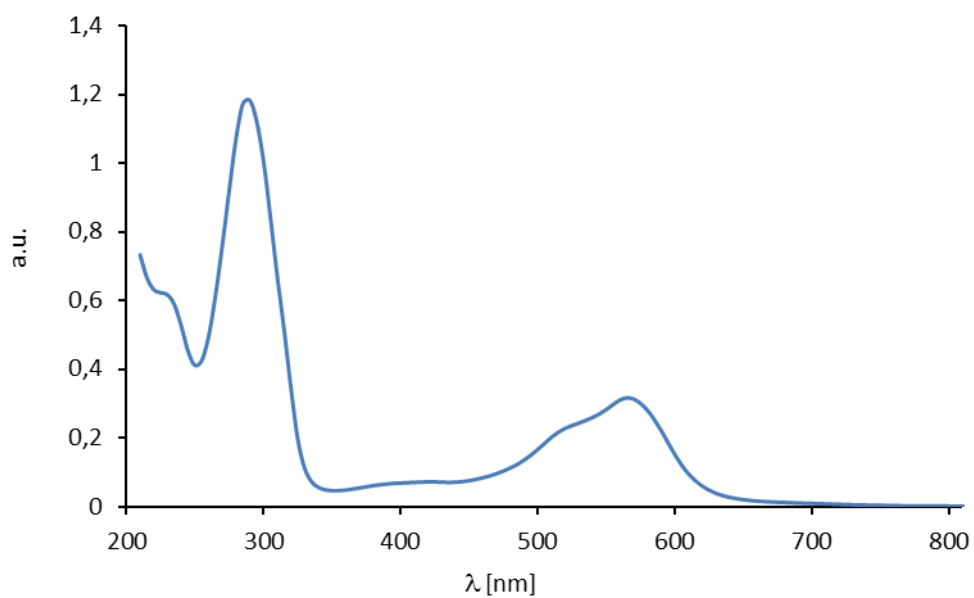
UV/Vis spectrum of **1**[SbF$_6$]$_2$ (50 μM in MeCN).
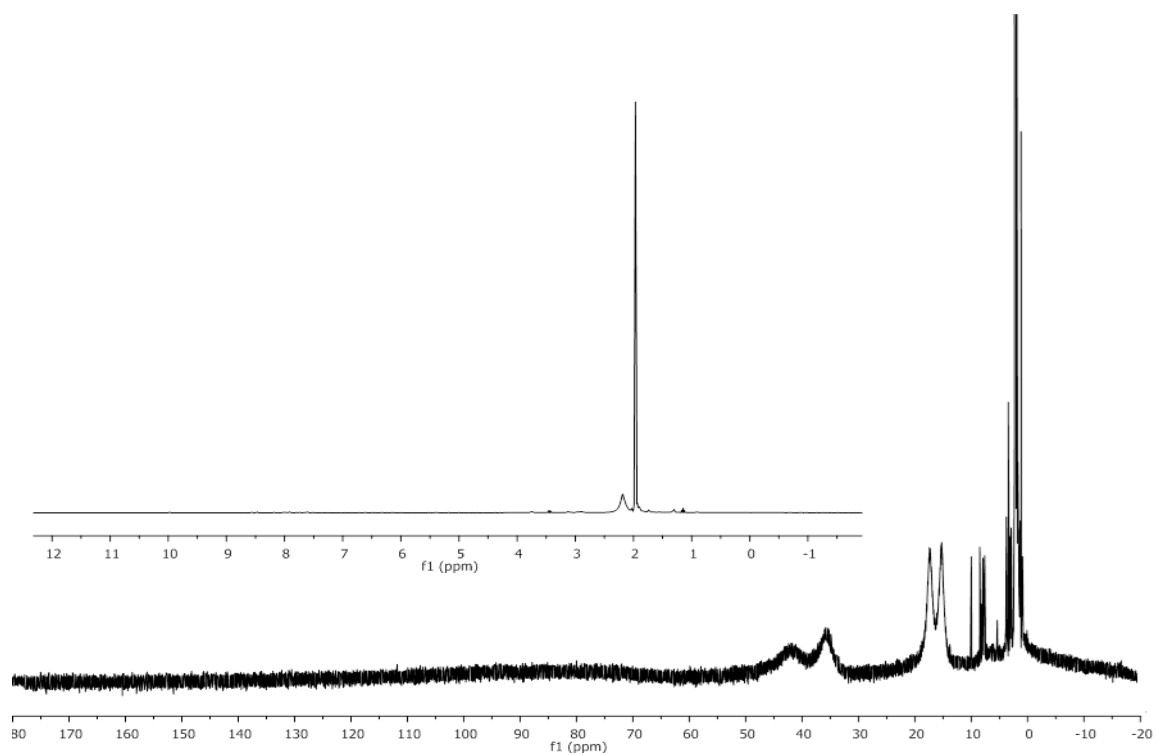
¹H-NMR of **1**[OTf]₂ (400.1 MHz, MeCN-*d₃*, 293 K)
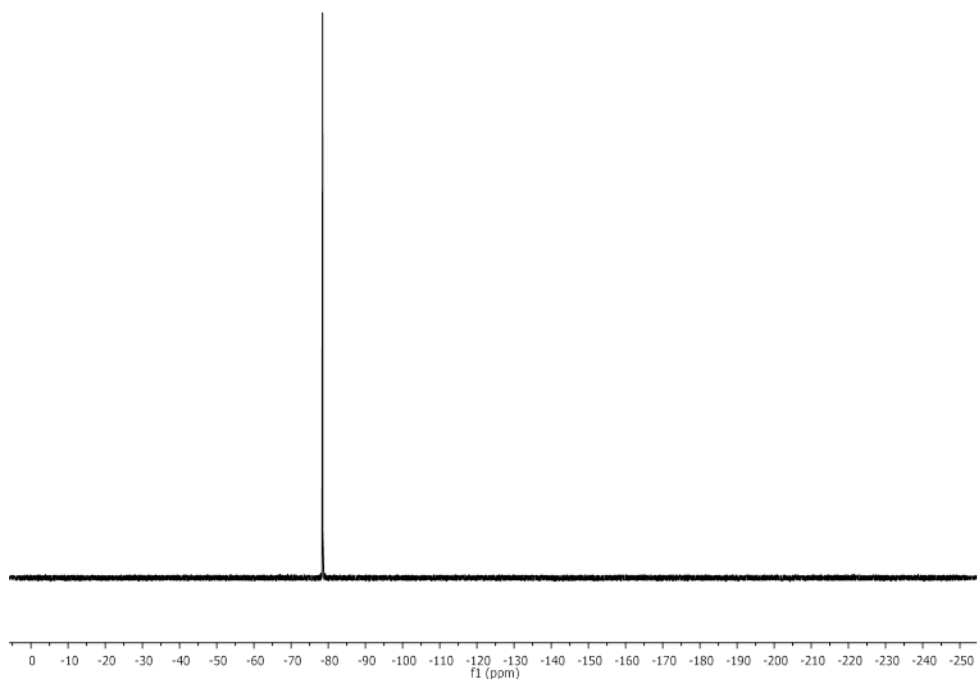
¹⁹F-NMR of **1**[OTf]₂ (282.4 MHz, MeCN-*d₃*, 293 K).

Pos. ESI-HRMS of **1**[*OTf*]$_2$
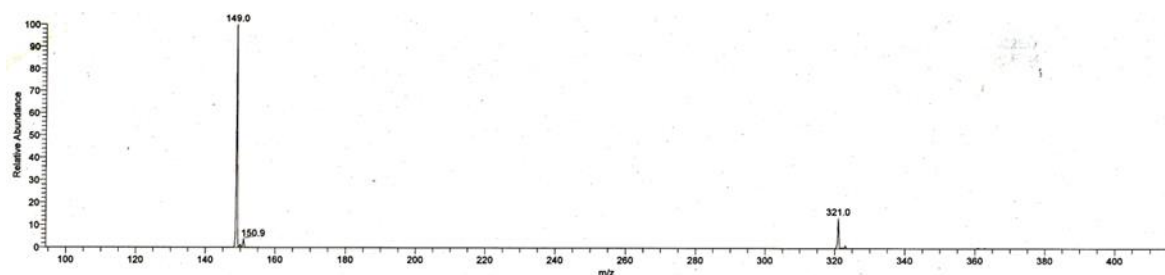
922EU #69-84 RT: 0.34-0.39 AV: 4 NL: 2.69E7
F: FTMS + p ESI Full ms [80.00-2000.00]

NL:
1.26E6
922EU#137 RT: 0.63 AV: 1
F: FTMS + p ESI Full ms
[80.00-2000.00]

NL:
5.86E5

C$_{18}$ H$_{21}$ FeN$_7$ S$_3$ (CF$_3$ SO$_3$):
C$_{19}$ H$_{21}$ Fe$_1$ N$_7$ S$_4$ O$_3$ F$_3$
pa Chrg 1

10
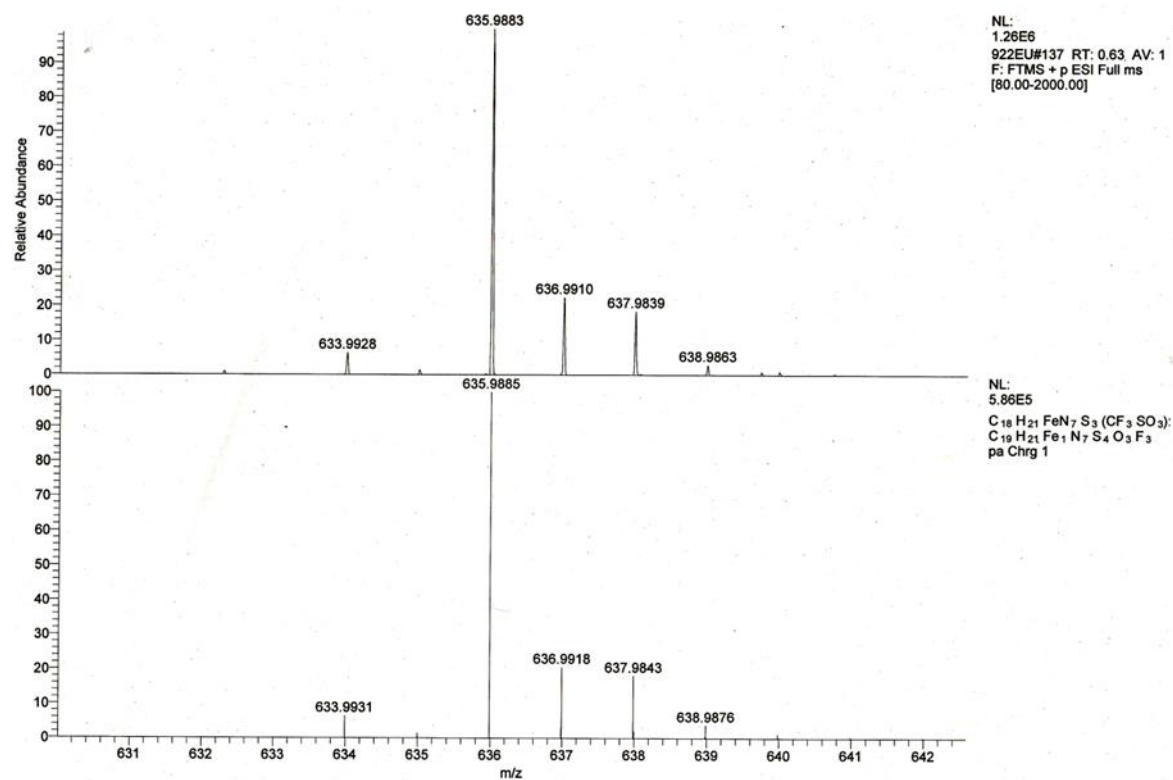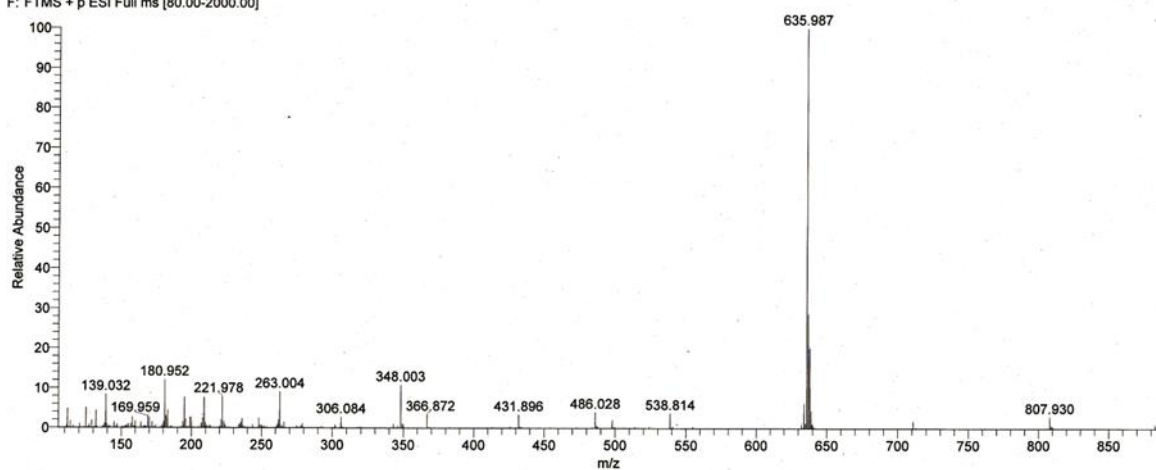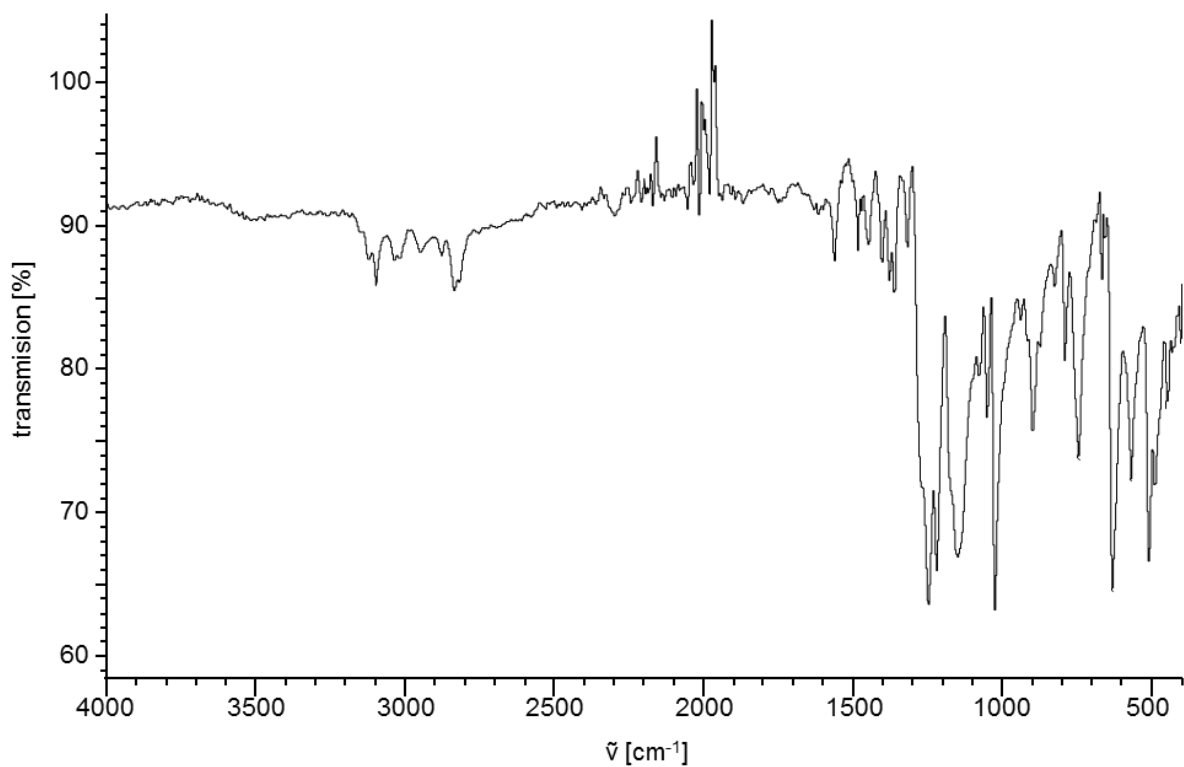
FT-IR of **1**[OTf]$_2$

UV/Vis of **1**[OTf]$_2$
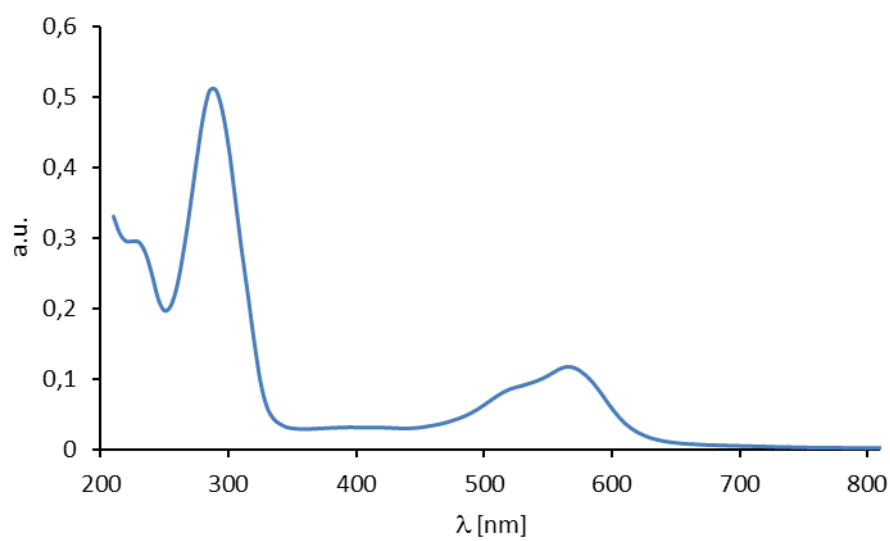
UV/Vis spectrum of **1**[OTf]$_2$ 50 μM in MeCN.
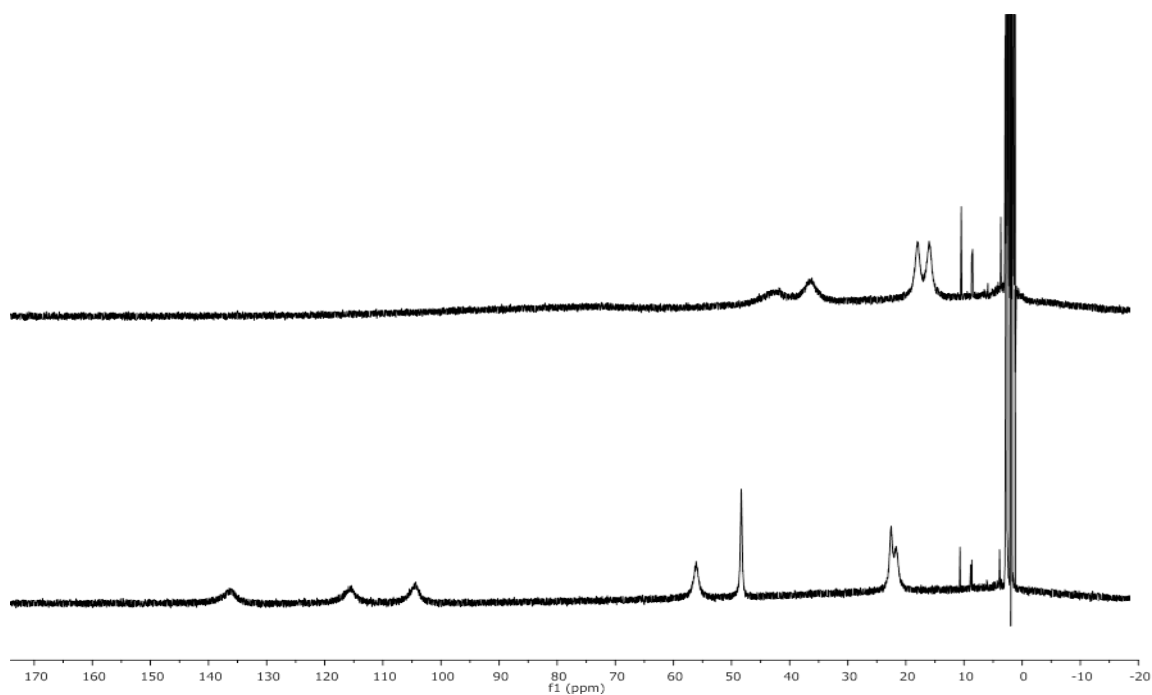
¹H-NMR of **1**[BF₄]₂ (300.1 MHz, MeCN-*d₃*): 293 K (top) and 340 K (bottom).

*¹⁹F-NMR of **1**[BF₄]₂*
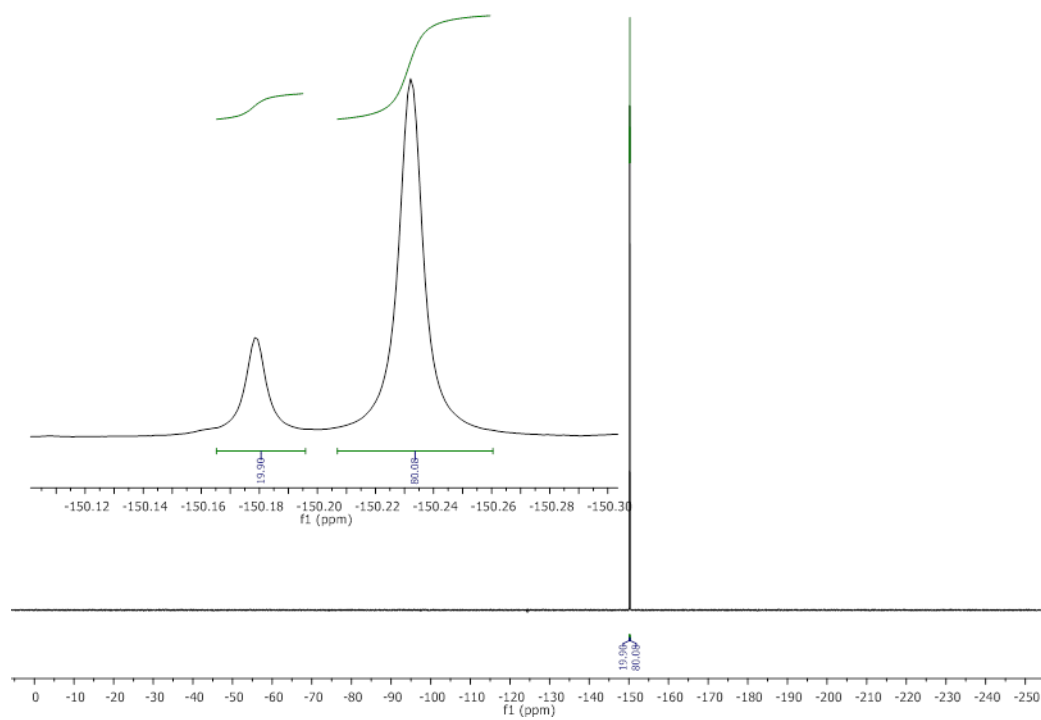
¹⁹F-NMR (282.4 MHz, MeCN-*d₃*, 293 K). Inset showing the typical boron isotope pattern.

Temperature dependent NMR of 1[BF₄]₂
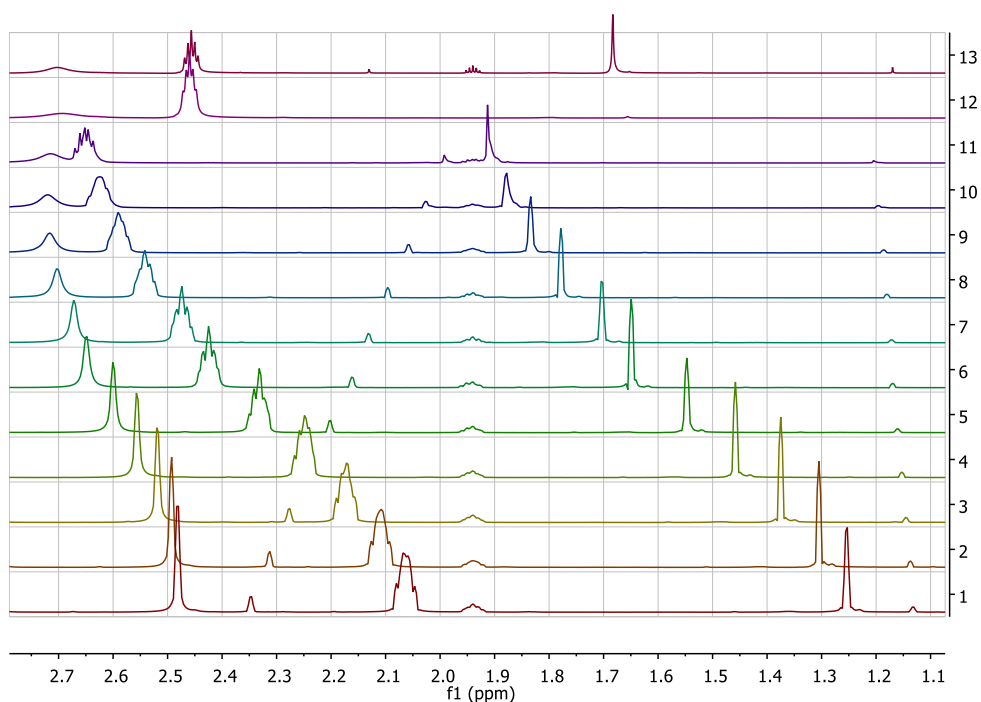
Temperature dependent ^{1}H-NMR of **1**[BF$_4$]$_2$ from 1.1 ppm to 2.8 ppm. From top to bottom: 400 MHz at 293K in MeCN-d_3 with 2 mM tBuOH with coaxial insert 2 mM tBuOH in MeCN-d_3, 400 MHz at 293 K in MeCN-d_3 without tBuOH and insert, then 340 K to 240 K in 10 K steps 300 MHz 200mM **1**[BF$_4$]$_2$ with 2 mM ^{t}BuOH and coaxial insert with 2 mM tBuOH in MeCN-d_3.
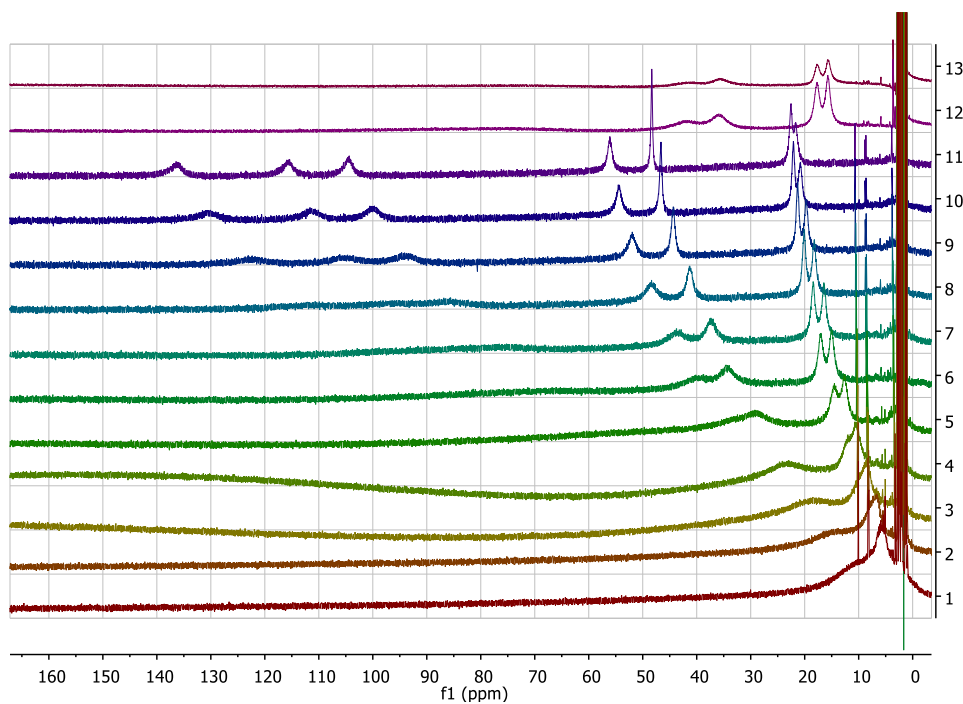
Temperature dependent ^{1}H-NMR of **1**[BF$_4$]$_2$ from −10 to 160 ppm. From top to bottom: 400 MHz at 293K in MeCN-d_3 with 2 mM tBuOH with coaxial insert 2 mM tBuOH in MeCN-d_3, 400 MHz at 293 K in MeCN-d_3 without tBuOH and insert, then 340 K to 240 K in 10 K steps 300 MHz 200 mM **1**[BF$_4$]$_2$ with 2 mM tBuOH and coaxial insert with 2 mM tBuOH in MeCN-d_3.
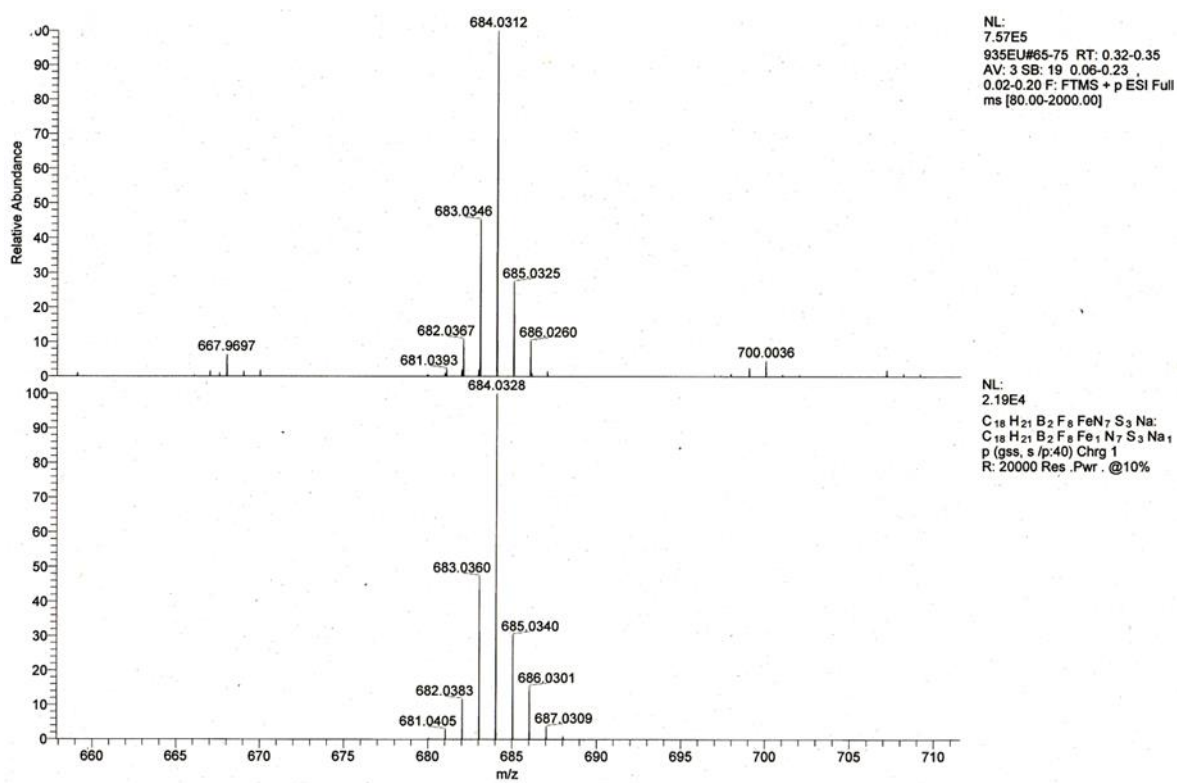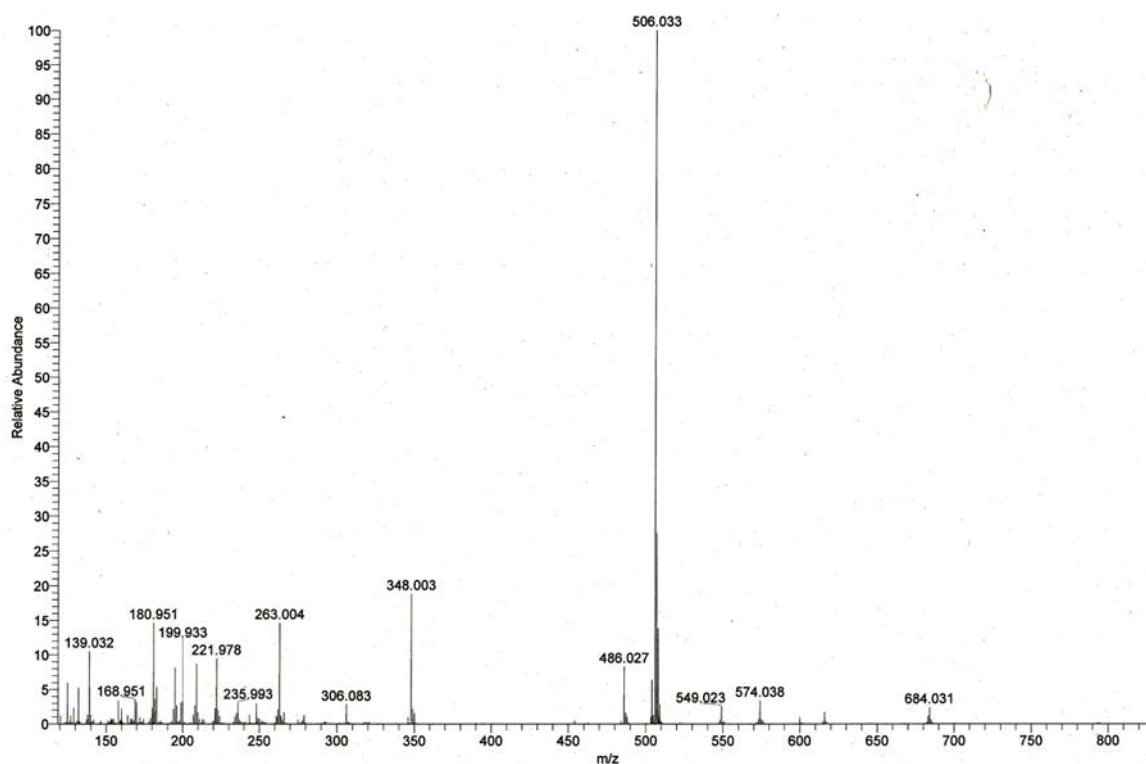
*FT-IR of **1**[BF₄]₂*
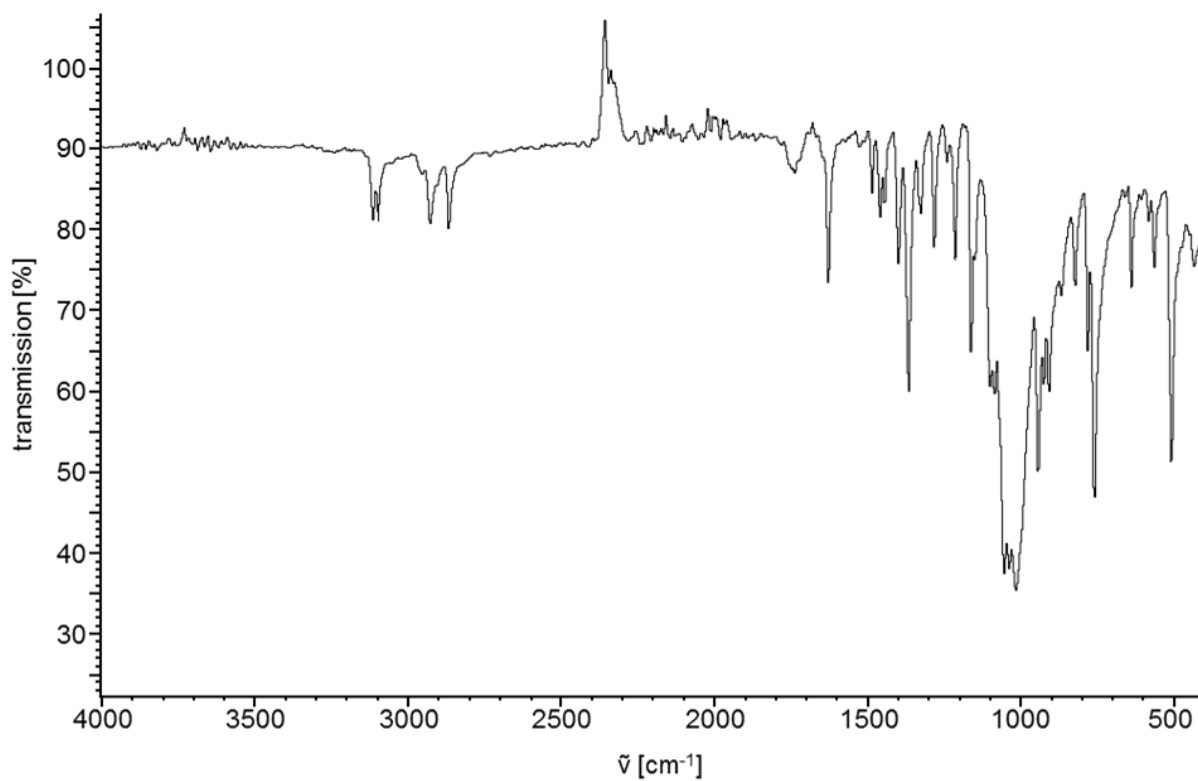
*UV/Vis of **1**[BF₄]₂*
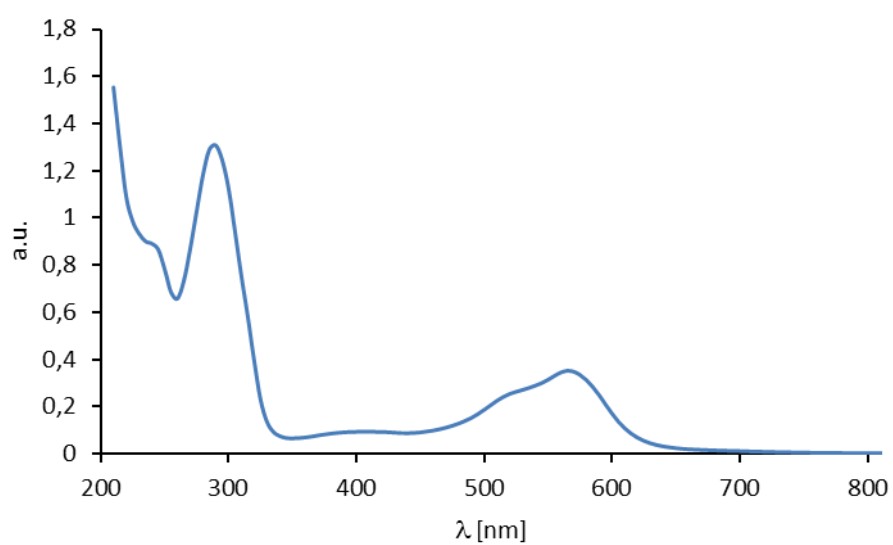
UV/Vis spectrum of **1**[BF$_4$]$_2$ 50 μM in MeCN.

Comparison of UV/Vis spectra
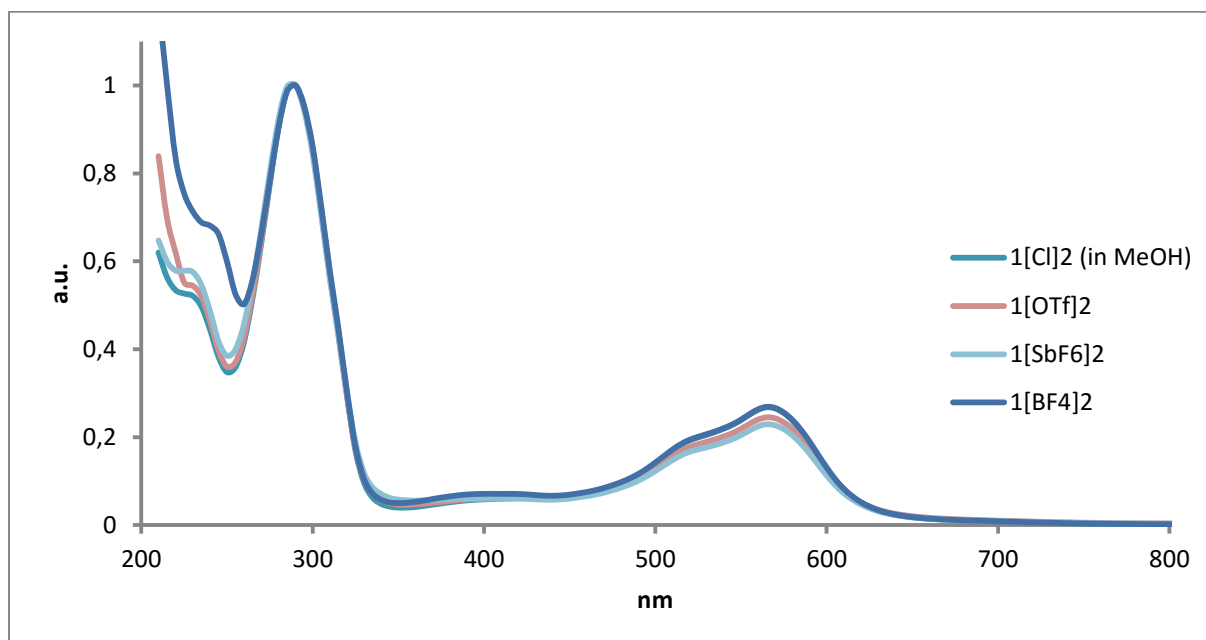
Normalized UV/Vis spectra of **1**[Cl]$_2$ 50 μM in MeOH, **1**[OTf]$_2$ 50 μM in MeCN, **1**[SbF$_6$]$_2$ 50 μM in MeCN, and **1**[BF$_4$]$_2$ 50 μM in MeCN.

DSC data on 1[BF₄]₂
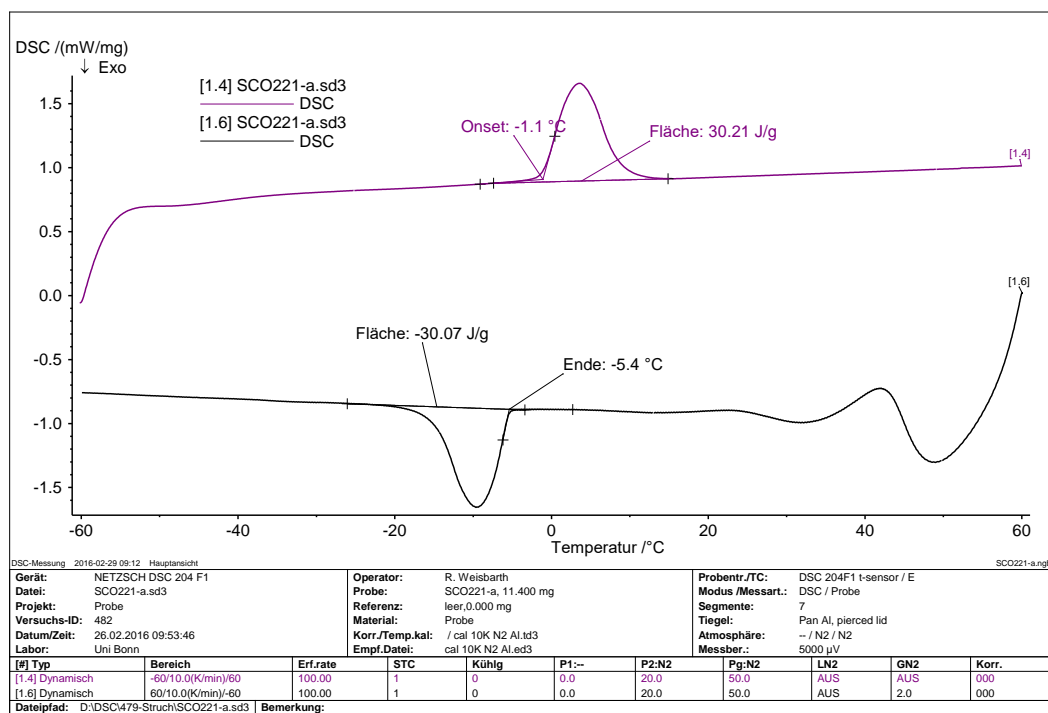
Thermal analyses were carried out on a Netzsch DSC 204 F1 equipped with a cooling device CC 200 F1 which allowed cooling with liquid nitrogen. 11.400 mg of the sample were weighed into aluminum crucibles, cold sealed and cooled from 60 °C to -60 °C and successively heated from -60 °C to 60 °C. The heating and cooling rates were 10 K/min. During the measurements, the oven was flushed with 20 ml/min nitrogen as protective gas and 50 ml/min nitrogen as purge gas.
The given temperatures correspond to the onset of a thermal effect.

Magnetic susceptibility measurements

Crystalline samples of **1**[BF$_4$]$_2$ (9.1727 mg), **1**[OTf]$_2$ (10.9846 mg), **1**[SbF$_6$]$_2$ (18.5599 mg) were used as obtained by the given synthetic procedures. They were slightly pressed to cylindrical shape and investigated in the temperature range from 1.9 K to 400 K at a vibrating frequency of 40 Hz in a magnetic field of 5000 Oe. A correction to the diamagnetic moment of the container was applied. The moment of the empty container was determined experimentally over the whole temperature range and susceptibility data of both the sample and the container were accordingly corrected.

Hysteresis loop in **1**[BF$_4$]$_2$ was investigated by variable temperature susceptibility measurements in a field of 5000 Oe, 10000 Oe and 20000 Oe at a scan rate of 1 K min^{-1}. It was also investigated at scan rates of 1 K min^{-1} and 0.25 K min^{-1} at 5000 Oe and 0.5 K min^{-1} at 20000 Oe.
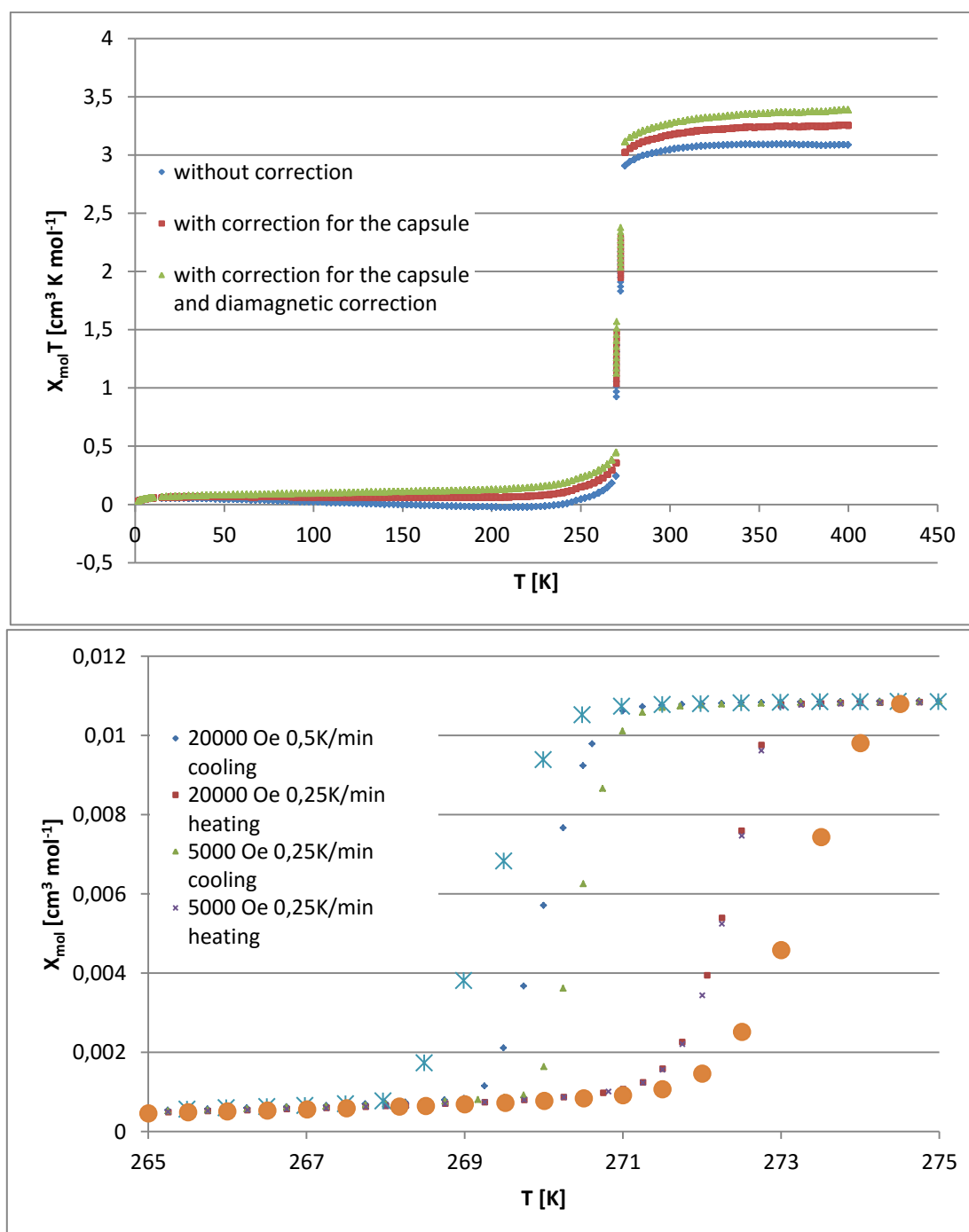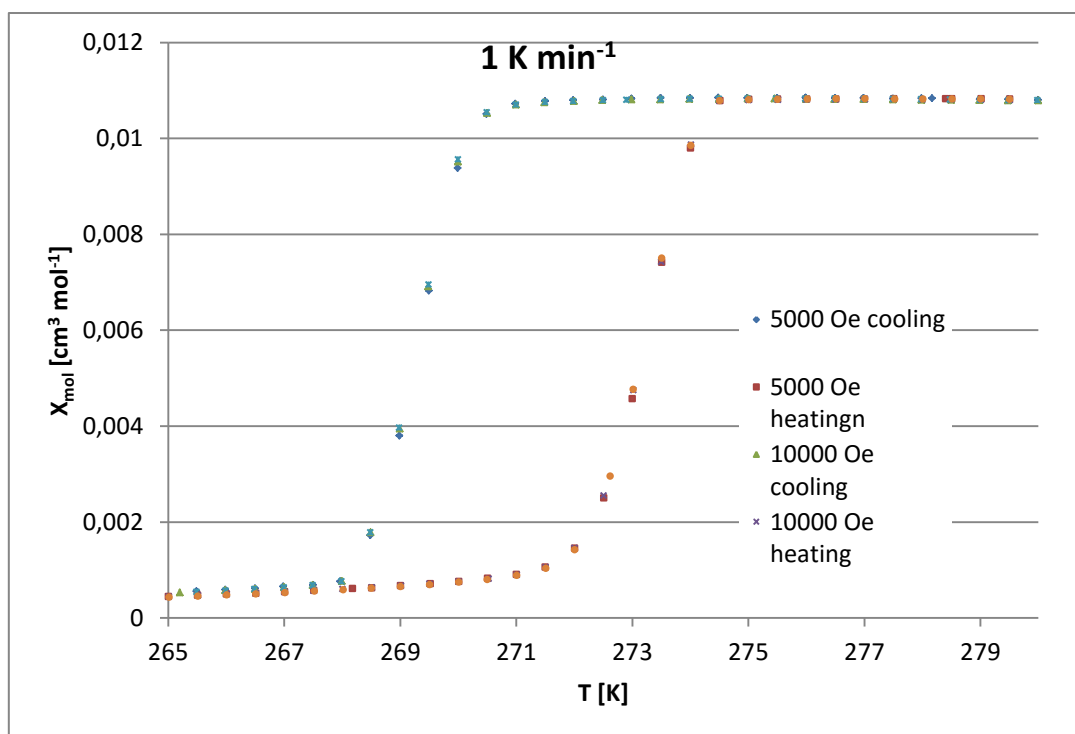
Magnetic data in solution were obtained by employing the Evans' method as described in literature[2] to the temperature dependent NMR-Data given above.

C = 0.02M	Δ *t*BuOH			Δ MeCN			
T	in Hz	μ_{Eff}	X_mT	in Hz	μ_{Eff}	X_mT	X_mT_{avg}
340	212,1	4,9101	2,9891	212,9000	4,9190	3,0000	2,9946
330	205,3	4,7621	2,8117	205,3000	4,7621	2,8117	2,8117
320	194,7	4,5715	2,5911	195,7000	4,5828	2,6039	2,5975
310	179,6	4,3288	2,3233	180,6000	4,3404	2,3357	2,3295
300	159,4	4,0229	2,0065	158,0000	4,0061	1,9898	1,9981
290	143,5	3,7630	1,7556	145,0000	3,7816	1,7730	1,7643
280	116	3,3456	1,3878	117,2000	3,3618	1,4012	1,3945
270	91	2,9361	1,0688	93,6000	2,9744	1,0969	1,0828
260	69	2,5417	0,8010	70,6000	2,5679	0,8176	0,8093
250	50,1	2,1659	0,5816	51,1000	2,1844	0,5916	0,5866
240	36,4	1,8561	0,4271	36,8000	1,8644	0,4310	0,4290

[2] D. F. Evans, *J. Chem. Soc.* **1959**, 2003.

Crystal structure data

Crystallographic data

	1[BF$_4$]$_2$ (high-spin)	**1**[BF$_4$]$_2$ (low-spin)	**1**[OTf]$_2$ (low-spin)	**1**[SbF$_6$]$_6$ (low-spin)
Molecular formula	C$_{18}$H$_{21}$B$_2$F$_8$FeN$_7$S$_3$	C$_{18}$H$_{21}$B$_2$F$_8$FeN$_7$S$_3$	C$_{18}$H$_{21}$F$_6$FeN$_7$S$_5$O$_6$	C$_{18}$H$_{21}$B$_2$F$_{12}$FeN$_7$S$_3$Sb$_2$
Crystal Class	Monoclinic	Monoclinic	Orthorhombic	Hexagonal
Space Group	P2$_1$/c	P2$_1$/c	Pca2$_1$	P6$_5$
a	16.356(2)	16.0951(5)	19.6249(5)	10.0709(9)
b	9.0081(10)	8.8292(2)	10.1650(3))	10.0709(9)
c	17.826(2)	17.4770(5)	14.9187(4)	49.888(4)
β	95.410(7)	93.211(2))	90	
γ				120
V (Å^3)	2614.8(5)	2479.90(12))	2976.09(14)	4381.9(9)
Z	4	4	4	6
T (K)	296	100	100	100
Radiation	Mo-Kα (λ = 0.71073)	Mo-Kα (λ = 0.71073)	Cu-Kα (λ = 1.54178 Å)	Mo-Kα (λ = 0.71073)
Measured reflections	71942	93559	40315	42543
Independent reflections	5122	4859	5313	7013
R$_{int}$	0.0507	0.0370	0.0696	0.00231
R$_1$ (I ≥ 2σ(I))	0.0606	0.0232	0.0518	0.0168
wR$_2$ (all data)	0.1701	0.0573	0.1436	0.0382
Goodness of fit	1.082	1.058	1.053	1.192
Flack parameter			0.006(6)	
CCDC No.	1496473	1496474	1496475	1496476

Clear reddish-brown plates of **1**[BF$_4$]$_2$ were obtained when the compound was crystallised from acetonitrile using *tert*-butyl methyl ether as antisolvent.

Clear black plank-like specimens of **1**[OTf]$_2$ were obtained when the compound was crystallised from acetonitrile using diethyl ether as antisolvent.

Clear yellow plates of **1**[SbF$_6$]$_2$ were obtained when the compound was crystallised from acetonitrile using diethyl ether as antisolvent.

The data collections for **1**[BF$_4$]$_2$ (high-spin), **1**[BF$_4$]$_2$ (low-spin) were performed on a Bruker Kappa ApexII diffractometer, the data collection of **1**[SbF$_6$]$_6$ (low-spin) was performed on a Bruker D8-Venture diffractometer. Mo-Kα irradiation (λ = 0.71073 Å) was used for the three samples. The diffractometer were equipped with a low-temperature device (Bruker Kryoflex I, Bruker AXS or Oxford Cryostream 800er series, Oxford Cryosystems). The data collection for **1**[OTf]$_2$ (low-spin) was performed on a Bruker D8-Venture diffractometer (area detector) using Cu-Kα irradiation (λ = 1.54178 Å). The diffractometer was equipped with a low-temperature device (Oxford Cryostream 800er series, Oxford Cryosystems).

Intensities were measured by fine-slicing ω and φ-scans and corrected for background, polarization and Lorentz effects. A semi-empirical absorption correction was applied for all data sets, except for that of **1**[OTf]$_2$ where a numerical absorption correction from face indices has been applied. The structures were solved by direct methods and refined anisotropically by the least-square procedure implemented in the SHELX program system.[3] Hydrogen atoms were included using the riding model on the bound carbon atoms.

---

[3]G. M. Sheldrick, *SHELXS97* and *SHELXL97*, University of Göttingen, Germany, **1997**.

CCDC numbers CCDC-1496473-1496476 contain the supplementary crystallographic data for this paper, which can be obtained free of charge from the Cambridge Crystallographic Data Centre via www.ccdc.cam.ac.uk/data_request/cif.

Crystallographic data
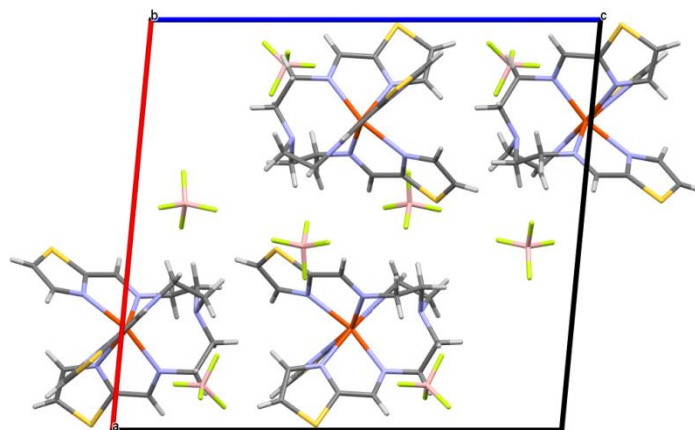
1[BF$_4$]$_2$

Unit cell of **1**[BF$_4$]$_4$ (high-spin) at 293 K. View along [010].
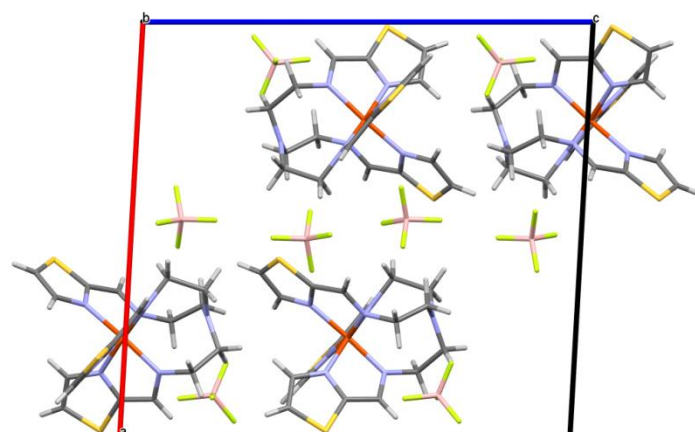
Unit cell of **1**[BF$_4$]$_2$ (low-spin) at 100 K. View along [010].
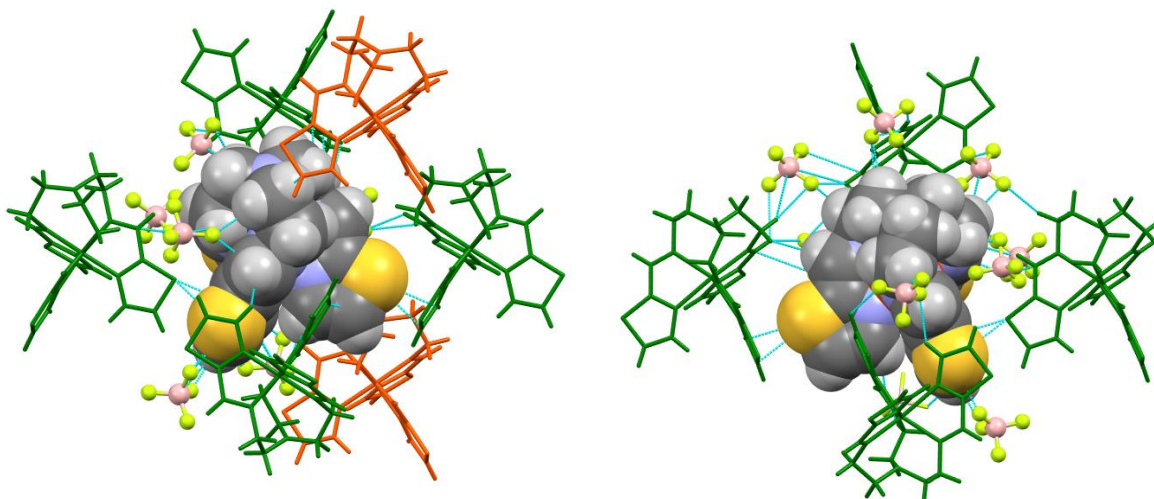
Comparison of the secondary coordination sphere in **1**[BF$_4$]$_2$ (left LS, 100 K, right HS, 293 K). Central cationic unit in space filling model, always connected cationic units green, contacts present only in the LS-state orange.

1[OTf]$_2$
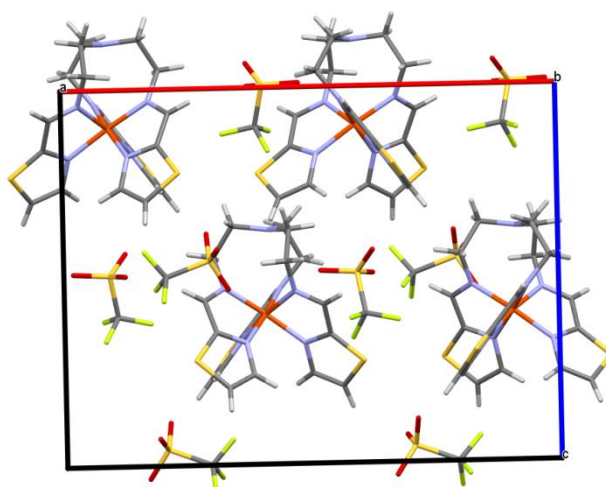
Unit cell of **1**[OTf]$_2$ (low-spin) at 100 K. View along [010].
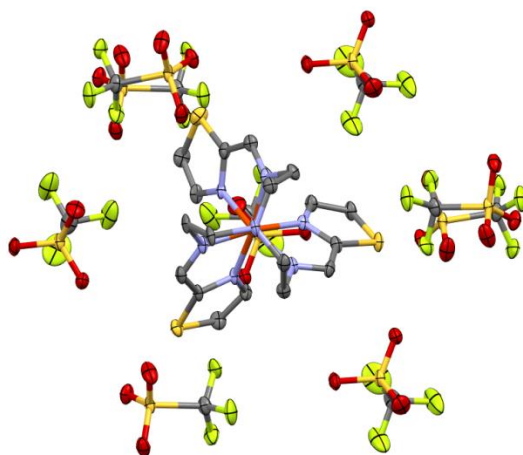
Secondary coordination sphere in **1**[OTf]$_2$ (low-spin) at 100 K. View along [001].

1[SbF$_6$]$_2$
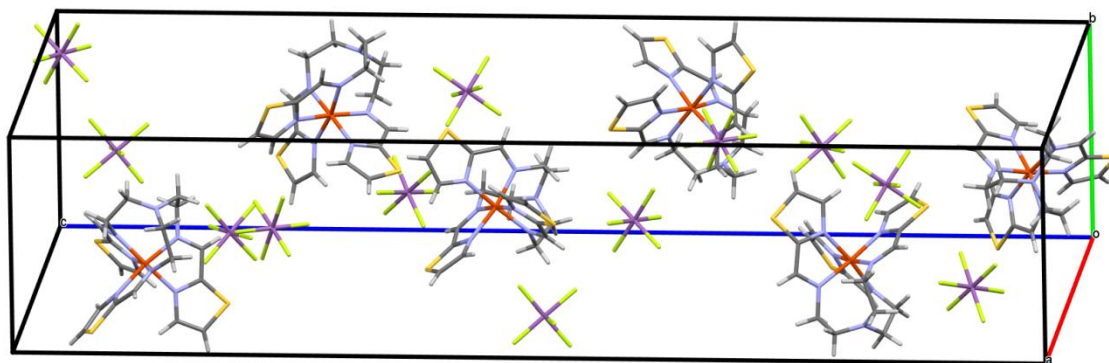
Unit cell of **1**[SbF$_6$]$_2$ (low-spin) at 100 K. Arbitrary view.
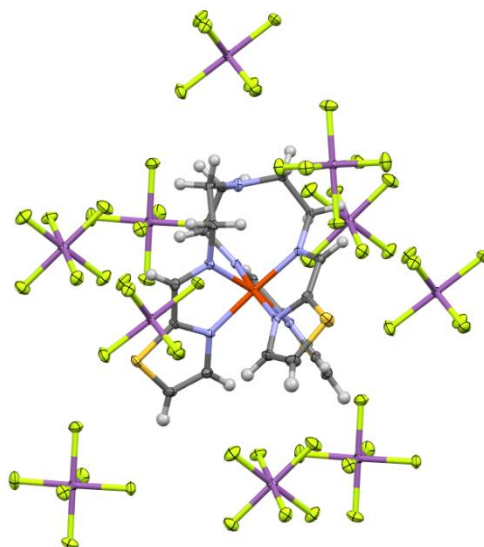
Secondary coordination sphere in **1**[SbF$_6$]$_2$ (low-spin) at 100 K. View along [111].

Analysis of coordination polyhedra via *Continuous Symmetry Measure* (CSM) and *Continuous Shape Measure* (CShM)

The coordination sphere of the complexes as revealed by XRD analysis were evaluated by employing the Continuous Symmetry Measure (CSM) and Continuous Shape Measure (CShM) programme developed by D. Avnir (http://www.csm.huji.as.il.

The SHAPE measure evaluates the degree of polyhedricity in distorted polyhedra. Perfect polyhedra are highly symmetric, and therefore in its application here, Shape is also a symmetry measure. The library of reference polyhedral shapes is large and includes the tetrahedron, octahedron, trigonal bipyramid, trigonal prism, and many more. The value of this measure ranges from zero - the molecule has the investigated polyhedral shape - to higher values (the upper limit is 100); the higher the shape-measure value, the farther is the structure from the reference shape.

	octahedron	trigonal prism
1[BF$_4$]$_2$ at 100 K	46.27	49.76
1[BF$_4$]$_2$ at 293 K	45.28*	
1[OTf]$_2$ at 100 K	43.18	47-12
1[SbF$_6$]$_2$ at 100 K	0.661	---

*the coordination polyhedron of **1**[BF$_4$]$_2$ in its high-spin form can best be described as a monocapped octahedron with six shorter Fe-N bonds and an elongated seventh bond.

24

Powder XRD data

X-Ray powder diffractograms were recorded at room temperature using Co-Kα_1 radiation and were baseline corrected. The experimental diffractograms were compared to the respective calculated diffraction patterns obtained from singly crystal XRD-data.

1[BF$_4$]$_2$
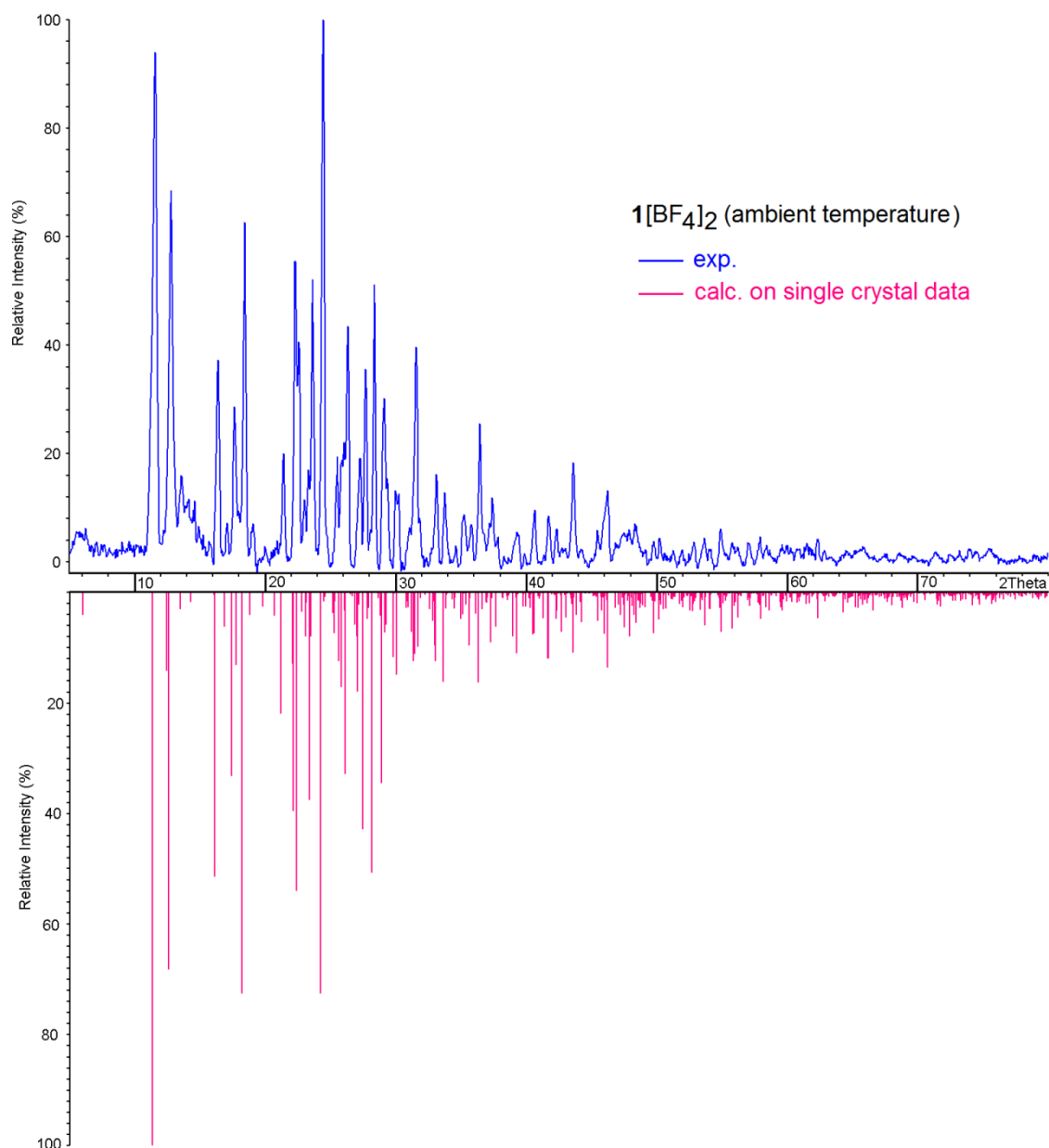
X-ray powder diffractogram of **1**[BF$_4$]$_2$, recorded at ambient temperature using Co-Kα_1 radiation. The experimental diffractogram (blue) is baseline corrected. The calculated diffraction pattern (violet) is shown as a line diagram.

1[OTf]₂
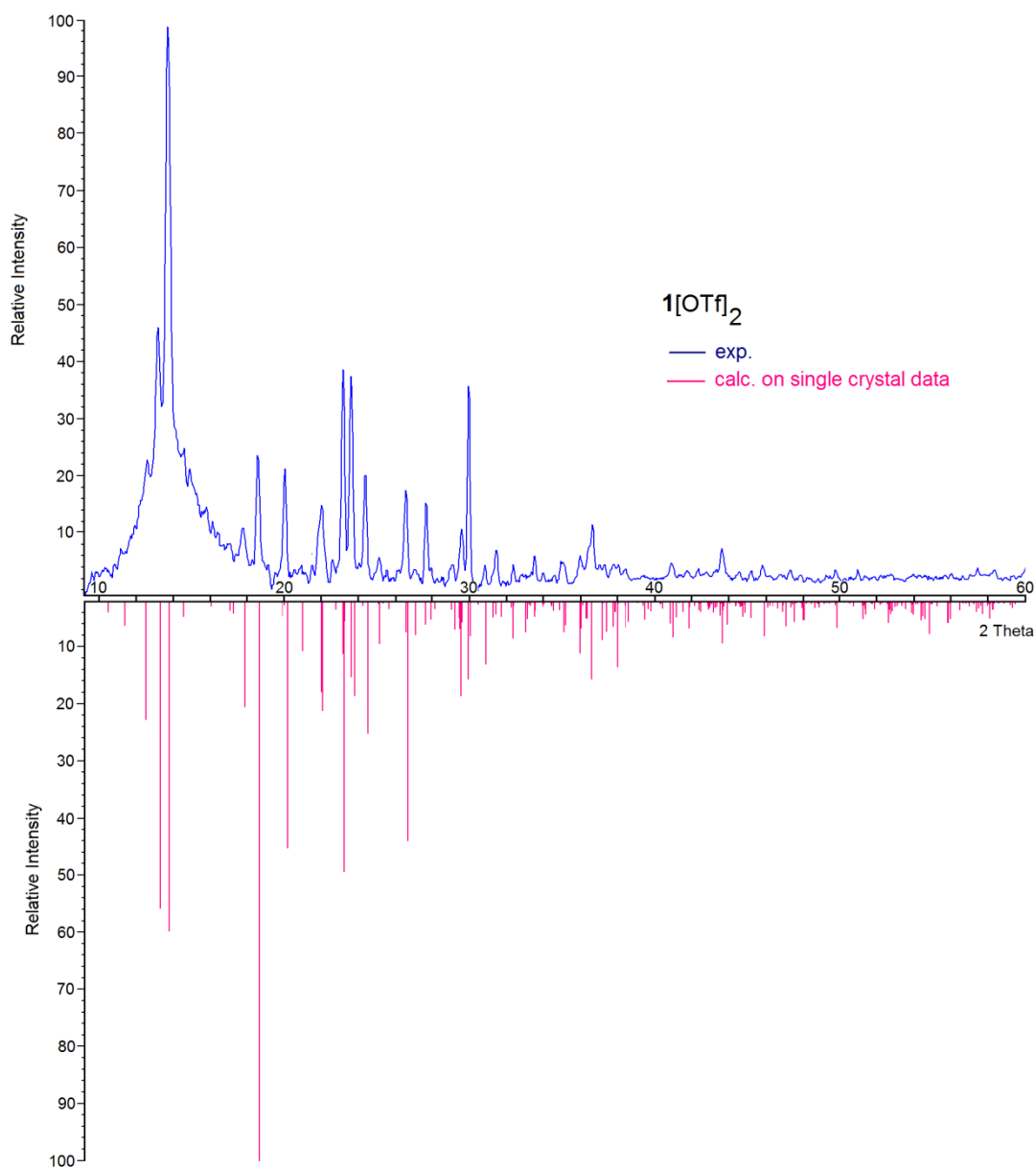
X-ray powder diffractogram of **1**[OTf]₂, recorded at ambient temperature using Co-Kα_1 radiation. The experimental diffractogram (blue) is baseline corrected. The calculated diffraction pattern (violet) is shown as a line diagram.

1[SbF$_6$]$_2$
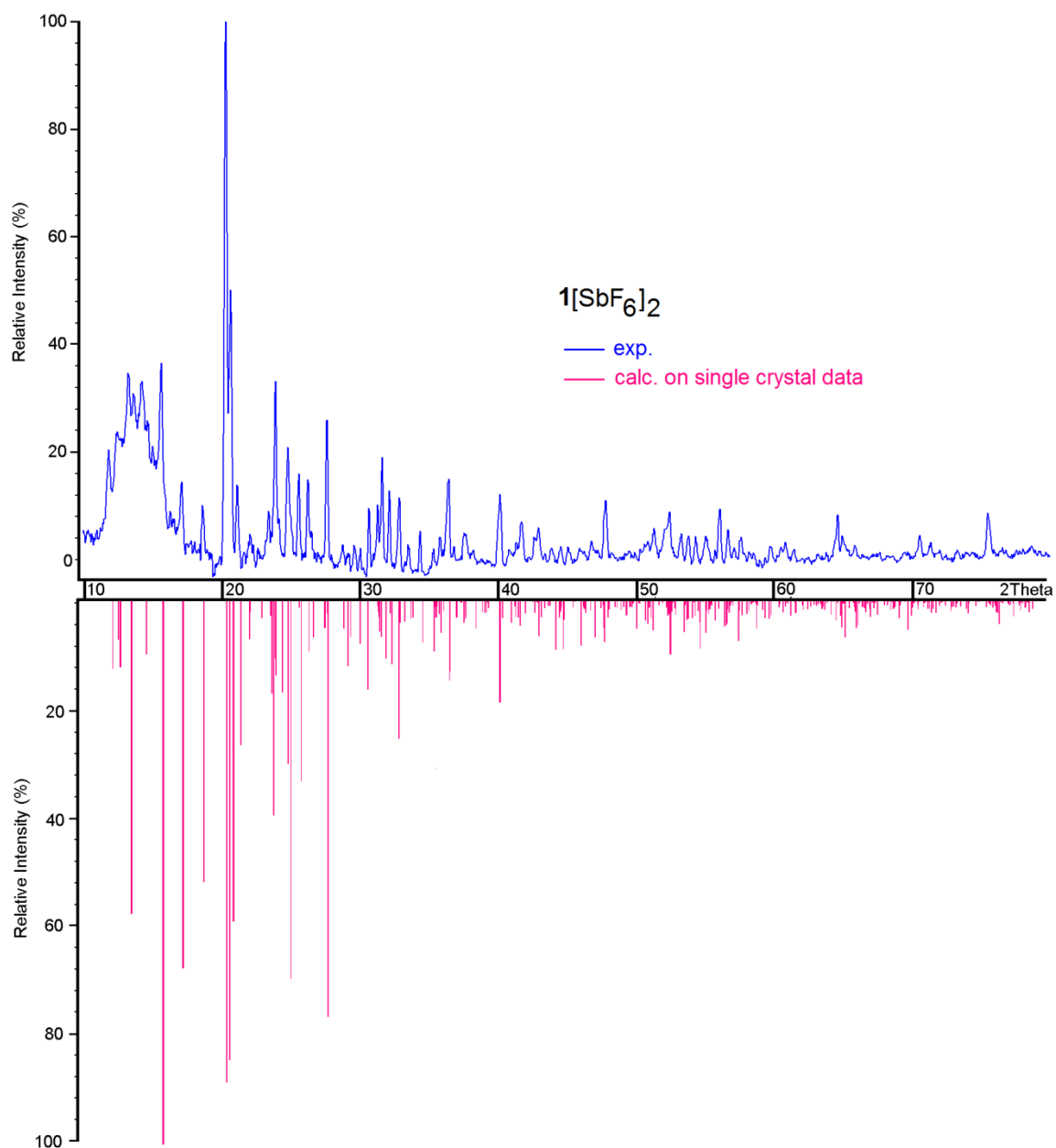
X-ray powder diffractogram of **1**[SbF$_6$]$_2$, recorded at ambient temperature using Co-Kα_1 radiation. The experimental diffractogram (blue) is baseline corrected. The calculated diffraction pattern (violet) is shown as a line diagram.